Amino Acids (2012) 42:2383–2391
DOI 10.1007/s00726-011-0980-5

ORIGINAL ARTICLE

The extended loop of the C-terminal carbohydrate-recognition domain of *Manduca sexta* immulectin-2 is important for ligand binding and functions

Xiu-Zhen Shi · Xiao-Qiang Yu

Received: 5 April 2011 / Accepted: 7 July 2011 / Published online: 30 July 2011

Abstract Our previous research showed that immulectin-2 (IML-2), a C-type lectin from the tobacco hornworm, *Manduca sexta*, is a pattern recognition receptor (PRR) that can bind to pathogen-associated molecular patterns (PAMPs), such as lipopolysaccharide (LPS), peptidoglycan (PG) and β-1,3-glucan, and IML-2 plays an important role in cellular encapsulation, melanization, phagocytosis, and prophenoloxidase (proPO) activation. Unlike most mammalian C-type lectins that contain a single carbohydrate-recognition domain (CRD), IML-2 is composed of tandem CRDs, and the C-terminal CRD2 contains an extended loop, which is not present in most C-type CRDs. We hypothesize that the extended loop may participate in ligand binding, encapsulation, melanization, phagocytosis and/or proPO activation in *M. sexta*. To test this hypothesis, two deletion mutant proteins (IML-$2^{\Delta 220-244}$ and IML-$2^{\Delta 220-257}$), in which the extended loop of the CRD2 was partially or completely deleted, were expressed and purified. By comparing the characteristics of recombinant IML-2, IML-$2^{\Delta 220-244}$ and IML-$2^{\Delta 220-257}$, we found that deletion of the extended loop in CRD2 impaired the ability of IML-2 to bind microbial PAMPs and to stimulate proPO activation, indicating that the extended loop of IML-2 plays an important role in ligand binding and biological functions.

Keywords Immulectin-2 · Carbohydrate-recognition domain · Extended loop · Ligand binding · Encapsulation and melanization · Prophenoloxidase activation

X.-Z. Shi · X.-Q. Yu (✉)
Division of Cell Biology and Biophysics, School of Biological Sciences, University of Missouri-Kansas City, 5007 Rockhill Road, Kansas City, MO 64110, USA
e-mail: Yux@umkc.edu

Introduction

Insects lack an adaptive immune system and mainly depend on the innate immune system to fight against microbial infections (Aggrawal and Silverman 2007; Cherry and Silverman 2006). Insect innate immune system shares similarities with the innate immune system of vertebrates (Kurata 2010), and is composed of cellular and humoral immune responses, such as phagocytosis, nodule formation, encapsulation and melanization, prophenoloxidase (proPO) activation and production of a variety of antimicrobial peptides (AMPs) (Lemaitre and Hoffmann 2007; Steiner 2004; Williams 2007).

Recognition of nonself pathogens by insect innate immune system is accomplished by germ line-encoded pattern recognition receptors (PRRs) (Hoffmann 2003). PRRs can recognize conserved molecular patterns, so-called pathogen-associated molecular patterns (PAMPs) such as bacterial lipopolysaccharide (LPS), peptidoglycan (PG) and fungal β-1,3-glucan, which are present on the pathogen surface but not on the host cells (Medzhitov and Janeway 2002; Pal and Wu 2009). Recognition of PAMPs by PRRs initiates cellular and humoral immune responses to protect the host (Pal and Wu 2009; Yu et al. 2002). Families of pattern recognition receptors (PRRs) have been identified in insects such as *Drosophila melanogaster*, *Bombyx mori* and *Manduca sexta* (Pal and Wu 2009). Lectins have been considered as one major family of PRRs in animal innate immune reaction as they can bind to glycoproteins and glycolipids on the surface of microorganisms (Takeuchi and Akira 2010).

It has been reported that animal calcium-dependent (C-type) lectins, which contain one or more carbohydrate-recognition domains (CRDs), can mediate pathogen

recognition and play an important role in pathogen clearance (Drickamer 1993; Weis et al. 1998; Hoffmann et al. 1999). In insects, multiple C-type lectin genes have been reported. More than 30 genes encoding C-type lectin domains have been found in *D. melanogaster*, and two of them were reported to act as PRRs in hemocyte encapsulation and melanization (Ao et al. 2007). Five C-type lectins (BmLBP, BmMBP, BmLEL-1, 2, and 3) have been reported in *B. mori* with functions in innate immune responses (Koizumi et al. 1999; Takase et al. 2009; Watanabe et al. 2006). In *Anopheles gambiae*, two C-type lectins have been reported to inhibit melanization of *Plasmodium berghei* ookinete and protect *A. gambiae* from Gram-negative bacterial infection (Osta et al. 2004; Schnitger et al. 2009). A C-type lectin was found in *Helicoverpa armigera* and was upregulated by bacteria, yeast and virus (Chai et al. 2008). Four C-type lectins named immulectins have been identified in the tobacco hornworm *M. sexta* and they participate in proPO activation, defense against Gram-negative bacterial infection, and in hemocyte encapsulation and melanization (Yu et al. 1999, 2005, 2006; Yu and Kanost 2000).

Immulectin-2 (IML-2) was first identified as an LPS-binding lectin induced in response to Gram-negative bacterial infection (Yu and Kanost 2000). Like other members of the immulectin group, IML-2 contains two CRDs, and the tandem CRD structure is unique to the immulectin group and differs from most animal C-type lectins that contain only a single CRD (Yu and Kanost 2003). IML-2 functions as a PRR and can stimulate immune responses in *M. sexta*, such as enhancing encapsulation and melanization, phagocytosis and stimulating proPO activation (Ling and Yu 2006a, b; Yu and Kanost 2000, 2003, 2004). Sequence alignment suggests that the N-terminal CRD1 of IML-2 is similar to mammalian mannose-binding lectin (MBL), while the C-terminal CRD2 is structurally similar to the CRD4 of the macrophage mannose receptor that contains an extended loop (Feinberg et al. 2000; Yu and Ma 2006). Our hypothesis is that the extended loop of CRD2 may participate in recognition of PAMPs and/or interaction with modulators/effectors to promote immune responses.

To test our hypothesis, two deletion mutant IML-2 proteins, IML-$2^{\Delta 220–244}$ and IML-$2^{\Delta 220–257}$ (in which the extended loop of CRD2 was partially (residues 220–244) or completely (residues 220–257) deleted), were expressed and purified. By comparing the abilities of three recombinant proteins (IML-2, IML-$2^{\Delta 220–244}$ and IML-$2^{\Delta 220–257}$) in ligand binding and in stimulation of cellular encapsulation and melanization, as well as in proPO activation, we confirm that the extended loop in the CRD2 of IML-2 is essential for recognition of PAMPs and biological functions.

Materials and methods

Insects and hemolymph collection

M. sexta eggs were bought from Carolina Biological Supply (Burlington, NC, USA), and larvae were reared with an artificial diet (Dunn and Drake 1983). Larvae in the second day of the fifth instar were used for experiments.

Hemolymph from individual naïve larvae was collected separately into microtubes on ice, and then centrifuged at 1,000×*g* for 10 min at 4°C to remove hemocytes. The individual hemocyte-free plasma samples were stored at −80°C for the following proPO activation assay.

Expression and purification of IML-2 and its two deletion mutant proteins

Recombinant wild-type IML-2 was expressed as described previously (Yu and Kanost 2003). Overlapping PCR was performed to obtain the templates for recombiannt expresssion of IML-$2^{\Delta 220–244}$ and IML-$2^{\Delta 220–257}$ (the numbering of residues is based on the mature IML-2 protein sequence). For IML-$2^{\Delta 220–244}$, primers IMLF (5′-CGA CCATGG ATG TGA ATT TTC-3′) and E220-244R (5′-ACC TGG AGC AAA TTT CAC AAA AGC CAT ATC TTT CCA AAA-3′) were used to amplify the 5′-end template, and primers IMLR (5′-TAT AAGCTT CCT AGT TTA CAT TTC-3′) and E220-244F (5′-GAT ATG GCT TTT GTG AAA TTT GCT CCA GGT GAG CCA -3′) were used to amplify the 3′-end template. For IML-$2^{\Delta 220–257}$, primers IMLF (5′-CGA CCATGG ATG TGA ATT TTC-3′) and E220-257R (5′-CCC GCC GCA GTA TTC CAC AAA AGC CAT ATC TTT CCA-3′) were used to amplify the 5′-end template, and primers IMLR (5′-TAT AAGCTT CCT AGT TTA CAT TTC-3′) and E220-257F (5′-GAT ATG GCT TTT GTG GAA TAC TGC GGC GGG GTT TAT-3′) were used to amplify the 3′-end template. DNA fragments of the 5′-ends and 3′-ends were purified separately and used as templates for overlapping PCR. The purified 5′-end and 3′-end templates of IML-$2^{\Delta 220–244}$ or IML-$2^{\Delta 220–257}$ were mixed to obtain the full length template by PCR with the following conditions: one cycle of 94°C for 2 min, five cycles of 94°C for 30 s, 56°C for 45 s and 72°C for 50 s. Then primer IMLF and IMLR were added into each PCR reaction to amplify the full length IML-$2^{\Delta 220–244}$ or IML-$2^{\Delta 220–257}$ with one cycle of 94°C for 2 min, 35 cycles of 94°C for 30 s, 56°C for 45 s and 72°C for 50 s, followed by one cycle of 72°C for 10 min.

Then the full length PCR fragments of IML-$2^{\Delta 220–244}$ and IML-$2^{\Delta 220–257}$ were purified and digested with *Nco*I/*Hind*III, purified and ligated into the *Nco*I/*Hind*III sites of the H6-pQE60 vector (Lee et al. 1994). Recombinant

IML-2, IML-$2^{\Delta 220–244}$ and IML-$2^{\Delta 220–257}$ were expressed in *Escherichia coli* XL1-blue cells after isopropyl-1-thio-β-D-galactopyranosid (IPTG, 1 mM) induction at 37°C overnight as described previously for recombinant IML-2 expression (Yu and Kanost 2003).

The recombinant wild-type IML-2, IML-$2^{\Delta 220–244}$ and IML-$2^{\Delta 220–257}$ were insoluble and were purified by nickel-nitrilotriacetic acid (Ni-NTA) resin (Qiagen) under denaturing conditions in 8 M urea, following the manufacturer's instructions. The purified proteins in 8 M urea were refolded by three-step dialysis in 25 mM Tris–HCl, 2 mM reduced glutathione, 0.4 mM oxidized glutathione and 5% glycerol, pH = 8.0, containing 3 and 1 M urea, respectively, and finally in 25 mM Tris–HCl and 5% glycerol, pH = 8.0 twice. Each dialysis step was carried out at 4°C overnight. The refolded proteins were stored at 4°C until use. The purified refolded proteins were verified by Western blot analysis using mouse monoclonal anti-polyHistidine antibody (Sigma) and polyclonal rabbit anti-IML-2 serum as the primary antibodies.

Circular dichroism (CD) spectrum analysis

CD spectra were obtained for recombinant IML-2, IML-$2^{\Delta 220–244}$ and IML-$2^{\Delta 220–257}$. The protein concentration was adjusted to 0.20 mg/ml in 25 mM Tris–HCl and 5% glycerol, pH = 8.0. The spectra were collected from 250 to 190 nm in a Jasco J-720 spectropolarimeter (Jasco corporation, Japan). A quartz cuvette with 1-mm light path was used to scan the sample in at least ten accumulations at 10 nm/min. Tris buffer (TB) (25 mM Tris–HCl, pH = 8.0) containing 5% glycerol was used as the control for the baseline. After subtracting the baseline, CD specrta were overlayed using spectrum analysis software (Jasco corporation, Japan).

Ligand binding assay

Flat-bottom 96-well microtiter plates (Nunc MaxiSorp, eBioscience) were coated with 2 μg/well of LPS-K12 (*E. coli* K12), LPS-0111:B4 (*E. coli* 0111:B4), PG-K12 (*E. coli* K12), PG-SA (*Staphylococcus aureus*), PG-BS (*Bacillus subtilis*), zymosan (*Saccharomyces cerevisiae*), mannan (*S. cerevisiae*) and laminarin (β-1,3-glucan) (50 μl/well of 40 μg/ml in water) as described previously (Yu and Kanost 2000; Yu and Ma 2006). Briefly, the purified recombinant IML-2, IML-$2^{\Delta 220–244}$ and IML-$2^{\Delta 220–257}$ were diluted in the binding buffer (50 mM Tris–HCl, 50 mM NaCl, pH = 8.0) containing 0.1 mg/ml BSA and 5 mM $CaCl_2$ to different concentrations, added to each well of the coated plates (50 μl/well) and incubated at room temperature for 3 h. The plates were washed with binding buffer four times (each for 5 min), and mouse monoclonal anti-polyHistidine antibody (Sigma, 1:3,000) was added (100 μl/well) and incubated at 37°C for 2 h. The plates were washed again, and then alkaline phosphatase-conjugated goat anti-mouse IgG (Sigma, 1:2,000 dilution in binding buffer containing 0.1 mg/ml BSA) was added (100 μl/well) and incubated at 37°C for another 2 h. Finally, 50 μl of *p*-nitro-phenyl phosphate (1 mg/ml in 10 mM diethanolamine, 0.5 mM $MgCl_2$) was added to each well and the plates were incubated for 20 min at room temperature. Absorbances at 405 nm for each well were measured by a plate reader (BioTek PowerWave XS Spectrophotometer). The absorbance data were collected and analyzed by the GraphPad software (GraphPad Software incorporated, California).

In vitro encapsulation and melanization

The nickel-nitrilotriacetic acid (Ni-NTA) agarose beads were washed with water and then with Tris-buffered saline (TBS) (25 mM Tris–HCl, 137 mM NaCl and 3 mM KCl, pH 7.0). The purified refolded proteins were dialyzed in TBS buffer overnight at 4°C and used to coat nickel beads at 4°C overnight. Coating of recombinant protein to nickel beads was performed as described previously until the beads were saturated with proteins (Ling and Yu 2006a). *M. sexta* CP36 protein (a His-tagged cuticle protein also expressed in bacteria and purified) (Suderman et al. 2003) was used as a control protein to coat the nickel beads. After the coating process was completed, the beads were washed with TBS buffer four times and stored at 4°C.

The encapsulation and melanization assays were performed as described previously (Ling and Yu 2006a; Yu et al. 2005). Briefly, 24-well plates were coated with 1% agarose. Forty microliters of hemolymph was collected from the second day of the fifth instar *M. sexta* larvae and mixed with 1.8 ml of Grace's cell culture media containing 50 μg/ml tetracycline. Then, 450 μl of the diluted hemolymph (containing hemocytes) was added to each well, and 1 μl of the protein-saturated (CP36, IML-2, IML-$2^{\Delta 220–244}$, and IML-$2^{\Delta 220–257}$) nickel beads was added to each well. The plates were shaken gently and stored at room temperature. Encapsulation and melanization of the beads were observed at 6, 24 and 48 h after addition of the beads. Hemolymph from four larvae was used for each experiment, and the experiments were repeated four times.

In vitro prophenoloxidase activation assay

Naïve plasma samples were screened for prophenoloxidase (proPO) activation as described previously (Ling et al. 2009). Plasma samples, which had low phenoloxidase activity when incubated alone but high phenoloxidase

activty after incubation with *Micrococcus luteus*, were selected for the following proPO activation assays.

Recombinant IML-2 (0.5 μg), IML-$2^{\Delta 220–244}$ (0.5 μg) or IML-$2^{\Delta 220–257}$ (0.5 μg) was incubated in Tris–Ca^{2+} buffer (100 mM Tris–HCl, 1 mM $CaCl_2$, 100 mM NaCl, pH = 7.5) in the absence or presence of TLRgrade LPS-K12 (0.5 μg) (Invivogen) at room temperature for 30 min. Two controls, buffer only (no protein or LPS) and LPS only (no protein), were also included in the assays. Then, 2 μl hemocyte-free plasma was added to each sample and incubated at room temperature for another 40 min. Finally, L-dopamine substrate (2 mM in 50 mM phosphate buffer, pH = 6.5, 200 μl) was added to every sample, and phenoloxidase (PO) activity was measured immediately at 470 nm by a plate reader at every minute for a total of 30 min. One unit of PO activity is defined as an increase of absorbance (ΔA_{470}) by 0.001 per minute. Each sample had four repeats, and the experiments were repeated at least three times. A representative set of data was used to make figures using a Graphpad software.

Results

Expression and purification of recombinant IML-2, IML-$2^{\Delta 220–244}$ and IML-$2^{\Delta 220–257}$

The full length cDNAs for IML-$2^{\Delta 220–244}$ and IML-$2^{\Delta 220–257}$ were obtained by overlapping PCR using IML-2 cDNA as a template, and the sequences of the three recombinant plasmid DNAs (H6-pQE60-IML-2, H6-pQE60-IML-$2^{\Delta 220–244}$ and H6-pQE60-IML-$2^{\Delta 220–257}$) were verified by DNA sequencing. Recombinant IML-2, IML-$2^{\Delta 220–244}$ and IML-$2^{\Delta 220–257}$ were expressed in *E. coli* XL1-blue after IPTG induction, purified under denaturing conditions in 8 M urea, and refolded by dialysis as described previously for IML-2 (Yu and Kanost 2003). SDS-PAGE analysis showed that the three recombinant proteins were purified to homogenetity (Fig. 1a), and the calculated molecular weights of IML-2, IML-$2^{\Delta 220–244}$ and IML-$2^{\Delta 220–257}$ were 36,057, 33,285 and 32,000 kDa, respectively. Western blot analysis showed that the three purified recombinant proteins could be recognized by monoclonal antibody against polyhistidine (Fig. 1b) and polyclonal antibody against IML-2 (Fig. 1c).

Deletion of the extended loop changes the contents of the secondary structures

The secondary structures of IML-2, IML-$2^{\Delta 220–244}$ and IML-$2^{\Delta 220–257}$ were determined by circular dichroism (CD) spectropolarimeter (Fig. 2). All three CD spectra showed a strong negative peak between 205 and 215 nm and one strong positive peak between 190 and 200 nm. The three CD spectra were similar, but not identical. Analysis of secondary structure contents in each CD spectrum showed that deletion of the extended loop decreased the contents of α-helix and β-strand by 2.5–7.5 and 12.5–16%, respectively, and increased the content of turns by 8–9%, but almost did not change the content of random coil (Table 1). These results suggest that deletion of the extended loop may cause changes in β-strands and turns in the carbohydrate-recognition domains (CRDs) of IML-2.

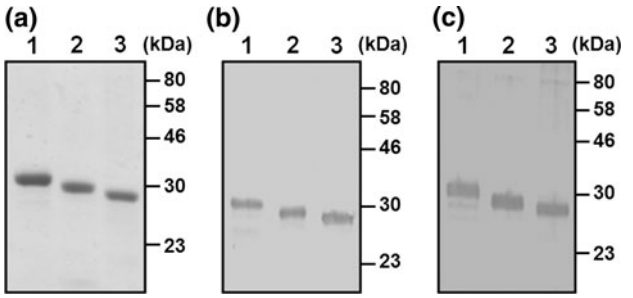

Fig. 1 SDS-PAGE gel analysis (**a**) and Western blot analysis (**b**, **c**) of the purified recombinant IML-2, IML-$2^{\Delta 220–244}$ and IML-$2^{\Delta 220–257}$. Purified refolded IML-2, IML-$2^{\Delta 220–244}$ and IML-$2^{\Delta 220–257}$ were separated on 12% SDS-PAGE and the proteins were either stained with Coomassie Brilliant Blue (**a**) or transferred to nitrocellulose membranes for Western blot analysis using monoclonal mouse anti-polyHistidine antibody (**b**) or rabbit polyclonal anti-IML-2 antibody (**c**). *Lanes 1–3* were purified recombinant IML-2, IML-$2^{\Delta 220–244}$ and IML-$2^{\Delta 220–257}$, respectively (2 μg each protein for the stained gel, and 50 ng each protein for Western blot)

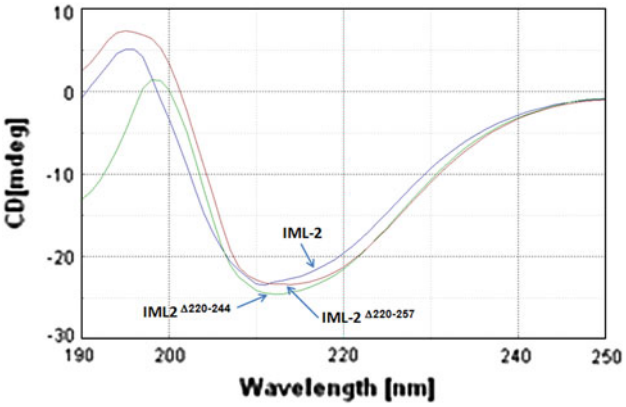

Fig. 2 Overlay of CD spectra from three recombinant IML-2 proteins. CD spectra were obtained from recombinant IML-2, IML-$2^{\Delta 220–244}$ and IML-$2^{\Delta 220–257}$ (at a concentration of 0.20 mg/ml in 25 mM Tris–HCl, 5% glycerol, pH = 8.0). Spectra were collected from 250 to 190 nm

The extended loop is important for ligand binding

In mammalian C-type lectins, an EPN (Glu-Pro-Asn) or QPD (Gln-Pro-Asp) motif in the CRD is important for

Table 1 CD spectrum

Fraction	Wild-type IML-2 (%)	IML-2$^{\Delta 220–244}$ (%)	IML-2$^{\Delta 220–257}$ (%)
Helix (ratio)	15.3	17.8	22.8
Beta (ratio)	39.6	27.1	23.6
Turn (ratio)	14.6	23.6	22.6
Random (ratio)	30.5	31.5	30.9

calcium binding and for the sugar binding specificity of mannose/glucose or galactose (Drickamer 1992). The extended loop in the CRD2 of IML-2 contains an EPN motif for binding to mannose/glucose, and it has been shown that IML-2 can bind to D-xylose, D-Glucose and mannan (Yu and Kanost 2000). Our previous works have shown that IML-2 has multiple functions, such as stimulation of proPO activation after binding to LPS (Yu and Kanost 2000), promotion in phagocytosis, encapsulation and melanization (Ling and Yu 2006a, b; Yu and Kanost 2004). We hypothesize that the extended loop of IML-2 may play an important role in interacting with different proteins and/or in ligand binding for its different functions. To test our hypothesis, we expressed and purified two IML-2 loop-deletion mutant proteins, IML-2$^{\Delta 220–244}$ and IML-2$^{\Delta 220–257}$. In IML-2$^{\Delta 220–257}$, the complete extended loop including the EPN (Glu^{250}-Pro^{251}-Asn^{252}) motif was deleted, while in IML-2$^{\Delta 220–244}$, most of the loop was deleted, but the EPN motif was retained. We first tested binding of IML-2, IML-2$^{\Delta 220–244}$ and IML-2$^{\Delta 220–257}$ to microbial cell wall components, such as LPS, PG, laminarin (β-1,3-glucan), zymosan and mannan, since binding of IML-2 to these ligands has already been demonstrated (Yu and Kanost 2000; Yu and Ma 2006). Plate ELISA assays showed that significantly more IML-2 than IML-2$^{\Delta 220–257}$ bound to all the eight ligands tested (except for LPS-K12 at 10nM protein concentration), including LPS and PG from Gram-negative *E. coli* K12 (LPS-K12 and PG-K12), LPS from *E. coli* 0111:B4 (LPS-0111), PG from Gram-positive *S. aureus* and *B. subtilis* (PG-SA and PG-BS), laminarin, zymosan, and mannan at both low (10 nM) and high (40 nM) protein concentrations (Fig. 3). At 10 nM protein concentration, significantly more IML-2 than IML-2$^{\Delta 220–244}$ bound to LPS-0111, PG-K12, PG-SA, laminarin and zymosan, while at 40 nM protein concentration, significantly more IML-2 than IML-2$^{\Delta 220–244}$ bound to all the seven microbial components but mannan (Fig. 3). Comparing IML-2$^{\Delta 220–244}$ with IML-2$^{\Delta 220–257}$, at 10nM protein concentration, significantly more IML-2$^{\Delta 220–244}$ than IML-2$^{\Delta 220–257}$ bound to the three PGs, laminarin and zymosan, whereas at 40 nM protein concentration, significantly more IML-2$^{\Delta 220–244}$ than IML-2$^{\Delta 220–257}$ bound to LPS-0111, PG-K12, PG-SA, laminarin and mannan (Fig. 3). These results suggest that the extended loop, including the EPN motif, in the CRD2 of IML-2 indeed is important for ligand binding.

The extended loop is not necessary for cellular encapsulation, but is essential for melanization

Previously, we showed that IML-2 can enhance hemocyte encapsualtion and melanization (Ling and Yu 2006a). To investigate the role of the extended loop in cellular encapsulation and melanization, we performed an in vitro encapsulation assay using IML-2, IML-2$^{\Delta 220–244}$ and IML-2$^{\Delta 220–257}$-coated nickel beads, and CP36 (an *M. sexta* cuticle protein)-coated beads were used as a control. At 6 h after incubation of the protein-coated beads with hemocytes, encapsulation was observed for IML-2, IML-2$^{\Delta 220–244}$ and IML-2$^{\Delta 220–257}$-coated beads (Fig. 4b–d), but not for CP36-coated beads (Fig. 4a). After incubation for 24 h, melanization of IML-2-coated beads were observed (Fig. 4h), a result consistent with our previous one (Ling and Yu 2006a), but melanization did not occur for IML-2$^{\Delta 220–244}$ and IML-2$^{\Delta 220–257}$-coated beads (Fig. 4f–h). At 48 h after incubation, melanization occurred to IML-2, IML-2$^{\Delta 220–244}$ and I-ML2$^{\Delta 220–257}$-coated beads (Fig. 4j–l). CP36-coated beads were neither encapsulated nor melanized at 6, 24 and 48 h after incubation with hemocytes (Fig. 4a, e, i). These results suggest that deletion of the extended loop did not affect the ability of IML-2 to enhance hemocyte encapsulation, but did have an impact on the ability of IML-2 to promote melanization.

The extended loop is essential for IML-2 to stimulate prophenoloxidase activation

Our previous works showed that IML-2 can bind to LPS to stimulate proPO activation, while IML-2 can also bind to mannan but does not activate proPO (Yu and Kanost 2000). We already showed that IML-2, IML-2$^{\Delta 220–244}$ and IML-2$^{\Delta 220–257}$ displayed differences in binding to microbial cell wall components (Fig. 3) and in enhancing hemocyte melanization (Fig. 4). Melanization of hemocyte-encapsulated beads is due to activation of proPO on the surface of hemocytes (Ashida and Brey 1998; Ling and Yu 2005). Thus, we test whether IML-2, IML-2$^{\Delta 220–244}$ and IML-2$^{\Delta 220–257}$ can stimulate proPO activation differently after binding to LPS. The in vitro proPO activation assay showed that addition of pure LPS (*E. coli* K12), the purified recombinant IML-2, IML-2$^{\Delta 220–244}$, or IML-2$^{\Delta 220–257}$ alone, or IML-2$^{\Delta 220–257}$/LPS mixture did not activate phenoloxidase (PO) in the plasma compared to the buffer control. However, after mixing with LPS, IML-2 stimulated PO activity to a significantly higher level than IML-2$^{\Delta 220–244}$, and IML-2$^{\Delta 220–244}$ activated PO to a

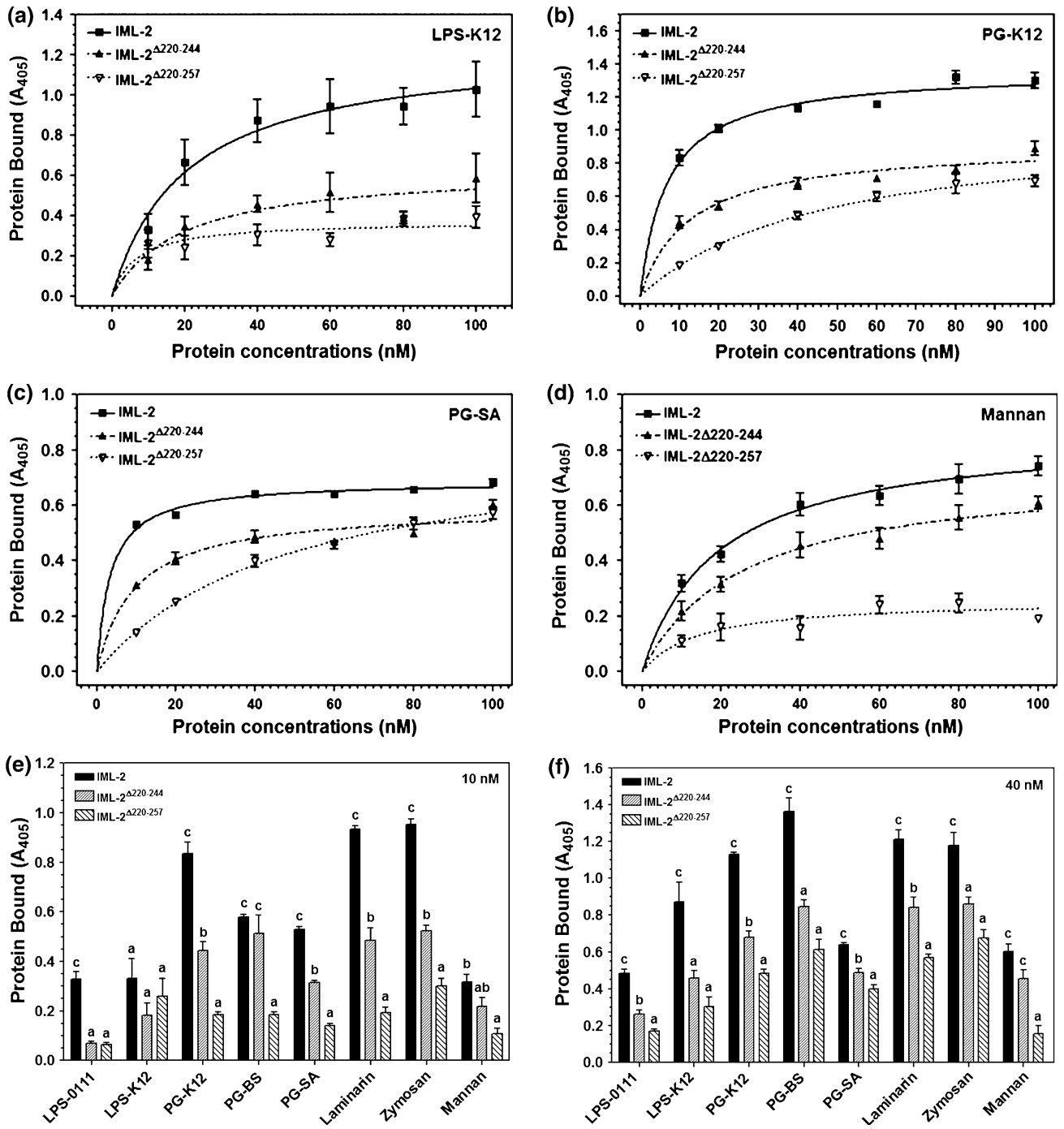

Fig. 3 Binding of recombinant IML-2, IML-$2^{\Delta 220-244}$ and IML-$2^{\Delta 220-257}$ to microbial cell wall components. The 96-well plates were coated with LPS-K12, LPS-0111:B4, PG-K12, PG-BS, PG-SA, laminarin, zymosan, or mannan. Recombinant IML-2, IML-$2^{\Delta 220-244}$ and IML-$2^{\Delta 220-257}$ were diluted to different concentrations in the binding buffer (50 mM Tris–HCl, 50 mM NaCl, pH = 8.0) containing 5 mM $CaCl_2$ and 0.1 mg/ml BSA, and then added to the microbial component-coated plates. Binding of recombinant proteins to each immobilized microbial component was determined by ELISA assay using anti-polyHistidine antibody. Each point or bar represents the mean of three individual measurements ± S.E.M. *Identical letters* indicate no significant difference among the three proteins for each ligand ($P > 0.05$), while *different letters* indicate significant difference among the three proteins ($P < 0.05$) determined by one-way ANOVA followed by a Tukey's multiple comparison test. (Significance was compared only among the three proteins for each ligand, so different letters could not be compared between different ligands)

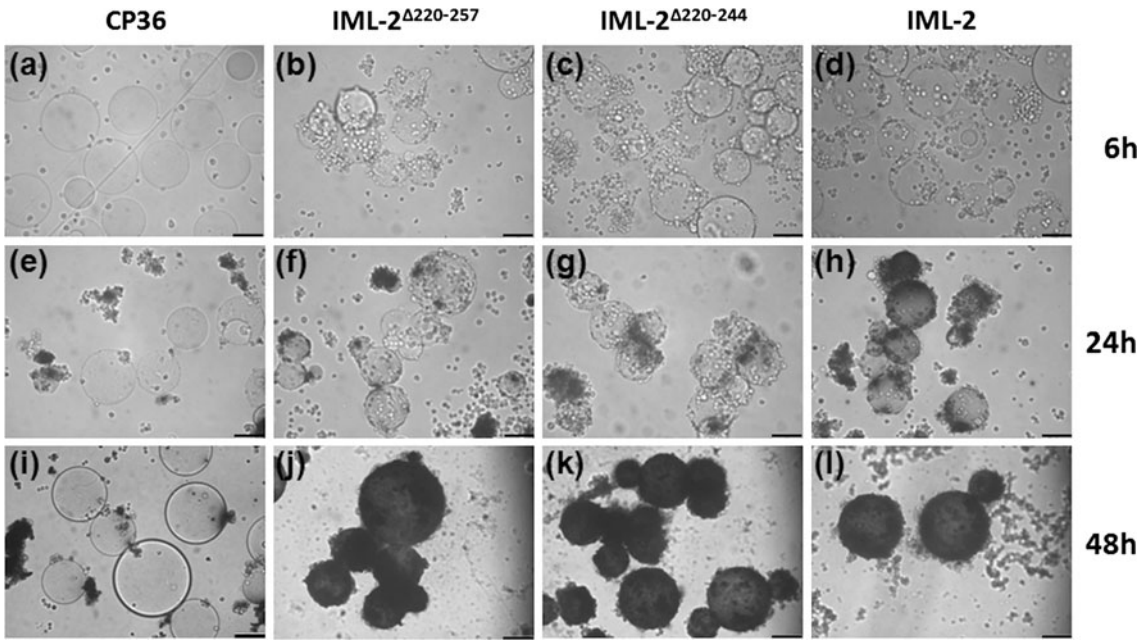

Fig. 4 IML-2, IML-$2^{\Delta 220–244}$ and IML-$2^{\Delta 220–257}$ enhance cellular encapsulation and melanization. Nickel agarose beads coated with recombinant His-tagged proteins (recombinant IML-2, IML-$2^{\Delta 220–244}$, IML$2^{\Delta 220–257}$ and CP36, a control protein) were incubated with hemolymph collected from the fifth instar naïve larvae at room temperature. The beads were observed by microscopy at 6 h (**a–d**), 24 h (**e–h**) and 48 h (**i–l**) after incubation. *Scale bar* is 200 μm

significantly higher level than IML-$2^{\Delta 220–257}$ (Fig. 5). These results suggest that the extended loop and the EPN motif are both essential for IML-2 to stimulate proPO activation.

Discussion

Immulectin-2 (IML-2) is a member of the C-type lectin superfamily first isolated and purified from *E. coli*-induced plasma of *M. sexta* larvae. Our previous works have demonstrated that IML-2 is a PRR that can recognize different microbial cell wall components, such as LPS, PG, β-1, 3-glucan (laminarin and curdlan) and mannan (Yu and Kanost 2000; Yu and Ma 2006), and stimulate a variety of immune responses, including stimulation of proPO activation and enhancing of phagocytosis, hemocyte encapsulation and melanization (Ling and Yu 2005, 2006a). One unique feature of IML-2 is that it contains tandem CRDs. The N-terminal CRD1 of IML-2 is structurally similar to the CRD of mammalian mannose-binding lectin (MBL) with two pairs of disulfide bonds, but lacks a few conserved residues for primary calcium binding, while the C-terminal CRD2 of IML-2 is more similar to the CRD4 of the macrophage mannose receptor with an extended loop and three pairs of disulfide bonds (Yu and Ma 2006). We think that the extended loop in the CRD2 of IML-2 may account for its ligand binding ability and/or different functions in

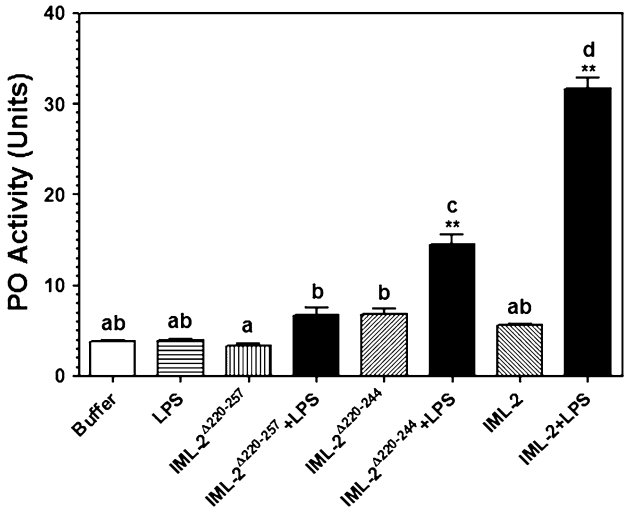

Fig. 5 Activation of prophenoloxidase by recombinant IML-2, IML-$2^{\Delta 220–244}$ and IML-$2^{\Delta 220–257}$. Recombinant IML-2 (0.5 μg), IML-$2^{\Delta 220–244}$ (0.5 μg) and IML-$2^{\Delta 220–257}$ (0.5 μg) were incubated with or without LPS-K12 (0.5 μg) at room temperature for 30 min. LPS-K12 only and buffer only (100 mM Tris–HCl, 1 mM $CaCl_2$, 100 mM NaCl, pH = 7.5) (without protein or LPS-K12) were used as controls. Then, 2 μl of plasma was added to each sample separately, and the mixture was incubated at room temperature for another 40 min. Finally, L-dopamine substrate (190 μl, 2 mM) was added to each sample. The PO activity was measured at 470 nm in a plate reader for 30 min. *Each bar* represents the mean of four individual measurements ±SEM. *Identical letters* indicate no significant difference between groups ($P > 0.05$), while *different letters* indicate significant difference between groups ($P < 0.05$) determined by one-way ANOVA followed by a Tukey's multiple comparison test

immune responses. To test our hypothesis, in this study, we expressed and purified two loop-deletion mutant IML-2 proteins (IML-$2^{\Delta 220–244}$ and IML-$2^{\Delta 220–257}$) and compared the wild-type IML-2 and two deletion mutant proteins in their ability to bind microbial cell wall components and to stimulate immune responses. IML-2, IML-$2^{\Delta 220–244}$ and IML-$2^{\Delta 220–257}$ were purified to homogeneity as shown by SDS-PAGE and Western blot analyses (Fig. 1). Deletion of the extended loop did not affect refolding of the two mutant proteins since IML-$2^{\Delta 220–244}$ and IML-$2^{\Delta 220–257}$ were refolded just like wild-type IML-2. The three recombinant proteins had similar CD spectra (Fig. 2), but deletion of the extended loop did have an effect on the contents of secondary structures, as the content of β-strands decreased in IML-$2^{\Delta 220–244}$ and IML-$2^{\Delta 220–257}$, while the content of turns increased (Table 1). Thus, deletion of the extended loop may not significantly change the core CRD structures of the two deletion mutant proteins, but may change the contents of loops and turns.

Our previous results have shown that IML-2 can bind to microbial components and IML-2 is localized on the surface of hemocytes (Yu and Kanost 2004; Yu and Ma 2006). These characteristics of IML-2 may account for its ability to enhance phagocytosis (Ling and Yu 2006b). Ligand binding assays showed that significantly less amounts of IML-$2^{\Delta 220–244}$ and IML-$2^{\Delta 220–257}$ than wild-type IML-2 bound to the eight microbial cell wall components tested, including *E. coli* LPS and PG, *S. aureus* and *B. subtilis* PG, laminarin, zymosan and mannan, and lesser amount of IML-$2^{\Delta 220–257}$ than IML-$2^{\Delta 220–244}$ bound to most ligands tested (Fig. 3). IML-$2^{\Delta 220–244}$ had most of the extended loop deleted, but retained the EPN (Glu^{250}-Pro^{251}-Asn^{252}) motif, which in mammalian CRD such as mannose-binding lectin (MBL), is important for ligand binding specificity of mannose/glucose, while IML-$2^{\Delta 220–257}$ had the complete extended loop including the EPN motif deleted. These results suggest that the extended loop in the CRD2 of IML-2 indeed is important for ligand binding. The EPN motif also contributes to ligand binding, as deletion of the EPN motif further decreases the amount of IML-$2^{\Delta 220–257}$ bound to some microbial components when compared with IML-$2^{\Delta 220–244}$ (Fig. 3). On comparing different microbial components, more IML-2 bound to laminarin and zymosan than mannan at both 10 and 40 nM protein concentrations (Fig. 3e, f), and more IML-2 bound to PG than LPS at 10 mM protein concentraton (Fig. 3e). Difference in IML-2 binding to two *E. coli* LPS (LPS-0111 and LPS-K12) was also observed at 40 nM protein concentration (Fig. 3f). Thus, the complete extended loop of IML-2 may play an important role in enhancing immune responses, such as phagocytosis, by binding to a variety of microbial cell wall components.

IML-2 can enhance hemocyte encapsulation and melanization (Ling and Yu 2006a). To do so, IML-2 must be able to interact with proteins/molecules on the surface of hemocytes to enhance encapsulation, and to stimulate proPO activation to enhance melanization. In vitro encapsulation and melanization assays showed that IML-2 and the two IML-2 deletion mutant proteins could all enhance hemocyte encapsulation. However, melanization was observed for the IML-2-coated beads at 24 h after incubation with hemocytes, but was not observed for the IML-$2^{\Delta 220–244}$ and IML-$2^{\Delta 220–257}$-coated beads until 48 h after incubation (Fig. 4). These results suggest that the extended loop of IML-2 is not responsible for enhancing hemocyte encapsulation, but is important for promotion of melanization. Melanization of hemocyte capsules requires activation of proPO, and it has been demonstrated that IML-2 can stimulate proPO activation (Ling and Yu 2005; Yu and Kanost 2000). Thus, we tested whether deletion of the extended loop has an impact on the ability of IML-2 to stimulate proPO activation. We used LPS as a ligand in proPO activation assay, because LPS by itself activated proPO slowly, but PG, zymosan and laminarin by themselves activated proPO rapidly (data not shown). We showed that addition of the three recombinant proteins or LPS alone, or IML-$2^{\Delta 220–257}$/LPS mixture to the plasma did not significantly activate PO activity compared to the buffer control, but IML-$2^{\Delta 220–244}$/LPS activated PO activity to a significantly higher level than the buffer control and IML-$2^{\Delta 220–257}$/LPS, and IML-2/LPS activated PO activity to a significantly higher level than IML-$2^{\Delta 220–244}$/LPS (Fig. 5). These results suggest that the extended loop including the EPN motif is essential for proPO activation. Deletion of the extended loop in IML-2 decreases its binding to LPS (Fig. 3), and may also impair its ability to interact with serine proteinase homologs (SPHs), proPO and/or proPO-activating proteinases (PAPs) to form a protein complex requried for proPO activation (Yu et al. 2003). To better understand the role of the extended loop of IML-2 in ligand binding and in protein interactions, three-dimensional structures of wild-type IML-2 and the loop-deletion mutant proteins are needed. Future work is needed to solve three-dimensional structures of IML-2 and loop-deletion mutant proteins, and to study structural and functional relationship of IML-2.

Acknowledgments This work was supported by National Institutes of Health Grant GM066356.

References

Aggrawal K, Silverman N (2007) Peptidoglycan recognition in Drosophila. Biochem Soc Trans 35:1496–1500

Ao J, Ling E, Yu XQ (2007) Drosophila C-type lectins enhance cellular encapsulation. Mol Immunol 44:2541–2548

Ashida M, Brey PT (1998) Recent advances in research on the insect prophenoloxidase cascade. In: Brey PT, Hultmark D (eds) Molecular mechanisms of immune responses in insects. Chapman Hall, London, pp 135–172

Chai LQ, Tian YY, Yang DT, Wang JX, Zhao XF (2008) Molecular cloning and characterization of a C-type lectin from the cotton bollworm, *Helicoverpa armigera*. Dev Comp Immunol 32:71–83

Cherry S, Silverman N (2006) Host–pathogen interactions in drosophila: new tricks from an old friend. Nat Immunol 7:911–917

Drickamer K (1992) Engineering galactose-binding activity into a C-type mannose-binding protein. Nature 360:183–186

Drickamer K (1993) $Ca2^{+}$-dependent carbohydrate-recognition domains in animal proteins. Curr Opin Struct Biol 3:393–400

Dunn PE, Drake D (1983) Fate of bacteria injected into naive and immunized larvae of the tobacco hornworm, *Manduca sexta*. J Invertebr Pathol 41:77–85

Feinberg H, Park-Snyder S, Kolatkar AR, Heise CT, Taylor ME, Weis WI (2000) Structure of a C-type carbohydrate recognition domain from the macrophage mannose receptor. J Biol Chem 275:21539–21548

Hoffmann JA (2003) The immune response of Drosophila. Nature 426:33–38

Hoffmann JA, Kafatos FC, Janeway CA, Ezekowitz RA (1999) Phylogenetic perspectives in innate immunity. Science 284:1313–1318

Koizumi N, Imamura M, Kadotani T, Yaoi K, Iwahana H, Sato R (1999) The lipopolysaccharide-binding protein participating in hemocyte nodule formation in the silkworm *Bombyx mori* is a novel member of the C-type lectin superfamily with two different tandem carbohydrate-recognition domains. FEBS Lett 443:139–143

Kurata S (2010) Extracellular and intracellular pathogen recognition by Drosophila PGRP-LE and PGRP-LC. Int Immunol 22: 143–148

Lee E, Linder ME, Gilman AG (1994) Expression of G-protein alpha subunits in *Escherichia coli*. Methods Enzymol 237:146–164

Lemaitre B, Hoffmann J (2007) The host defense of *Drosophila melanogaster*. Annu Rev Immunol 25:697–743

Ling E, Yu XQ (2005) Prophenoloxidase binds to the surface of hemocytes and is involved in hemocyte melanization in *Manduca sexta*. Insect Biochem Mol Biol 35:1356–1366

Ling E, Yu XQ (2006a) Cellular encapsulation and melanization are enhanced by immulectins, pattern recognition receptors from the tobacco hornworm *Manduca sexta*. Dev Comp Immunol 30:289–299

Ling E, Yu XQ (2006b) Hemocytes from the tobacco hornworm *Manduca sexta* have distinct functions in phagocytosis of foreign particles and self dead cells. Dev Comp Immunol 30:301–309

Ling E, Rao XJ, Ao JQ, Yu XQ (2009) Purification and characterization of a small cationic protein from the tobacco hornworm *Manduca sexta*. Insect Biochem Mol Biol 39:263–271

Medzhitov R, Janeway CA Jr (2002) Decoding the patterns of self and nonself by the innate immune system. Science 296:298–300

Osta MA, Christophides GK, Kafatos C (2004) Effects of mosquito genes on *Plasmodium* development. Science 303:2030–2032

Pal S, Wu LP (2009) Lessons from the fly: pattern recognition in *Drosophila melanogaster*. Adv Exp Med Biol 653:162–174

Schnitger AK, Yassine H, Kafatos FC, Osta MA (2009) Two C-type lectins cooperate to defend *Anopheles gambiae* against Gram-negative bacteria. J Biol Chem 284:17616–17624

Steiner H (2004) Peptidoglycan recognition proteins: on and off switches for innate immunity. Immunol Rev 198:83–96

Suderman RJ, Andersen SO, Hopkins TL, Kanost MR, Kramer KJ (2003) Characterization and cDNA cloning of three major proteins from pharate pupal cuticle of *Manduca sexta*. Insect Biochem Mol Biol 33:331–343

Takase H, Watanabe A, Yoshizawa Y, Kitami M, Sato R (2009) Identification and comparative analysis of three novel C-type lectins from the silkworm with functional implications in pathogen recognition. Dev Comp Immunol 33:789–800

Takeuchi O, Akira S (2010) Pattern recognition receptors and inflammation. Cell 140:805–820

Watanabe A, Miyazawa S, Kitami M, Tabunoki H, Ueda K, Sato R (2006) Characterization of a novel C-type lectin, *Bombyx mori* multibinding protein, from the *B. mori* hemolymph: mechanism of wide-range microorganism recognition and role in immunity. J Immunol 177:4594–4604

Weis WI, Taylor ME, Drickamer K (1998) The C-type lectin superfamily in the immune system. Immunol Rev 163:19–34

Williams MJ (2007) *Drosophila hemopoiesis* and cellular immunity. J Immunol 178:4711–4716

Yu XQ, Kanost MR (2000) Immulectin-2, a lipopolysaccharide-specific lectin from an insect, *Manduca sexta*, is induced in response to gram-negative bacteria. J Biol Chem 275:37373–37381

Yu XQ, Kanost MR (2003) *Manduca sexta* lipopolysaccharide-specific immulectin-2 protects larvae from bacterial infection. Dev Comp Immunol 27:189–196

Yu XQ, Kanost MR (2004) Immulectin-2, a pattern recognition receptor that stimulates hemocyte encapsulation and melanization in the tobacco hornworm, *Manduca sexta*. Dev Comp Immunol 28:891–900

Yu XQ, Ma Y (2006) Calcium is not required for immulectin-2 binding, but protects the protein from proteinase digestion. Insect Biochem Mol Biol 36:505–516

Yu XQ, Gan H, Kanost MR (1999) Immulectin, an inducible C-type lectin from an insect, *Manduca sexta*, stimulates activation of plasma prophenol oxidase. Insect Biochem Mol Biol 29:585–597

Yu XQ, Zhu YF, Ma C, Fabrick JA, Kanost MR (2002) Pattern recognition proteins in *Manduca sexta* plasma. Insect Biochem Mol Biol 32:1287–1293

Yu XQ, Jiang H, Wang Y, Kanost MR (2003) Nonproteolytic serine proteinase homologs are involved in prophenoloxidase activation in the tobacco hornworm, *Manduca sexta*. Insect Biochem Mol Biol 33:197–208

Yu XQ, Tracy ME, Ling E, Scholz FR, Trenczek T (2005) A novel C-type immulectin-3 from *Manduca sexta* is translocated from hemolymph into the cytoplasm of hemocytes. Insect Biochem Mol Biol 35:285–295

Yu XQ, Ling E, Tracy ME, Zhu Y (2006) Immulectin-4 from the tobacco hornworm *Manduca sexta* binds to lipopolysaccharide and lipoteichoic acid. Insect Mol Biol 15:119–128